

# A Genetic Algorithm for Designing Uncoded Space-Time Labelling Diversity Mappers

Sulaiman Saleem Patel, Tahmid Quazi, Hongjun Xu

School of Engineering: Discipline of Electrical, Electronic and Computer Engineering  
University of Kwa-Zulu Natal, Durban, South Africa

**Abstract**—The extent to which Uncoded Space-Time Labelling Diversity is able to improve the error performance of space-time block coded (STBC) systems is dependent on the binary mappers used to encode information. Existing design techniques are limited; as they either rely on symmetry-based heuristics, or constrain the size of the constellation due to high computational costs. This paper proposes a new genetic algorithm for labelling diversity (LD) mapper design which is applicable to constellations of any shape or size. The proposed algorithm is tested using 16QAM, 64QAM, 32PSK and three 16APSK constellations that do not display diagonal symmetry. The proposed LD mappers match the best heuristic designs for 16QAM and 64QAM. The 32PSK LD mapper produced achieves a diversity gain of  $\approx 8$ dB when compared to the available heuristic-based LD mapper. In addition, the 16APSK mappers achieve a diversity gain of approximately 3 to 8dB compared to Alamouti-coded STBC systems for the three non-symmetric constellations considered.

**Index Terms**—genetic algorithms, labelling diversity, mapper design, MIMO communication, quadratic assignment problem

## I. INTRODUCTION

Uncoded Space-Time Labelling Diversity (USTLD) [1] is a recent technique proposed to improve the performance of space-time block coded (STBC) wireless systems in the presence of multipath fading. USTLD systems reduce the bit error rate (BER) of the STBC system by adopting a multiple-input, multiple-output (MIMO) structure and implementing labelling diversity (LD).

Prior to its application in STBC systems in [1], the idea of LD (sometimes referred to as Mapping Diversity in literature) was initially proposed for bit-interleaved coded systems with iterative decoding [2]–[4]. The use of convolutional coding in these systems increases the power consumption, detection complexity and latencies experienced; which prompted studies of LD applied to uncoded systems [1]. Apart from the STBC systems of [1], relevant literature on the use of LD includes its application to decode-and-forward relay systems [5] and multi-packet data transmissions with automatic repeat requests (ARQs) [6]. Other works expanding on STBC applications of LD include studies of spatial modulation [7], media-based modulation using RF mirrors [8], antenna correlation [9], detection complexity [10] and signal-space diversity [11].

In USTLD systems, LD is achieved by using pairs of symbols from constellations with different binary mappings to encode each information codeword. These symbol pairs are then transmitted across two time slots. For the transmission of a single codeword using an  $M$ -ary constellation, there

are  $M$  possible symbol pairs that could be transmitted over these two time slots. However, the receiver is able to detect a total of  $M^2$  possible combinations of symbols. Since only  $M$  combinations out of the  $M^2$  possible combinations are valid, the error performance is improved.

The extent to which LD is achieved depends on the binary mappings of each constellation. The end-goal of a mapper design is to ensure that adjacent symbols on each constellation are spaced further apart than in the base constellation. [1] suggests a design metric for these mapping structures, as well as symmetry-based heuristic techniques to design mappers for square  $M$ -ary quadrature amplitude modulation (MQAM) and  $M$ -ary phase shift keying (MPSK) systems. Other heuristic-based mappers have been designed in [5] for 16QAM and 64QAM. The reliance on heuristics for these mapper designs constrains the constellations that may be applied to USTLD systems.

Other LD works propose algorithmic approaches to mapper design, such as the 16QAM mapper design algorithm for convolutionally coded systems in [4]. A more general approach to LD mapper design is found in [6], wherein mapper design is shown to be an instance of the quadratic assignment problem (QAP). [6] shows that for a system requiring  $\kappa$  LD mappers, there are  $(M!)^\kappa$  possible solutions to the QAP, where  $(\cdot)!$  represents the factorial. Due to the enormity of the search space, [6] uses a lower-bound approximate QAP solver that iteratively finds  $\kappa$  optimal LD mappers solutions one at a time, thereby reducing the problem search space to  $M! \times \kappa$ . Even after reducing the search space, [6] reports that their algorithm is still too computationally expensive for larger constellations, where  $M > 16$ .

In summary, the current approaches to designing USTLD systems have the following limitations: i) the existing symmetry-based heuristics for mapper design are inapplicable to asymmetric constellations and may not necessarily produce good mappers for symmetrical ones, and ii) the existing algorithms for mapper design are computationally expensive and infeasible for  $M > 16$ . In order to overcome these limitations, this paper proposes a new approach to mapper design based on genetic algorithms (GAs) [12]. GAs are a robust heuristic approach to solving large-scale, combinatorial optimisation problems, based on the biological process of “natural selection” [13]. They have previously been used in mapper design applications for amplitude PSK (APSK) [14]–[16] and to solve instances of the QAP [13], [17]. By

basing the proposed algorithm on a GA design, it will be able to produce LD mappers for constellations unconstrained by the modulation order or possible asymmetry.

In terms of notation, this paper represents vectors and scalars in boldface and italics respectively.  $\|\cdot\|$  represents the Frobenius norm of a vector, and  $|\cdot|$  represents the absolute value of a scalar.

## II. SYSTEM MODEL

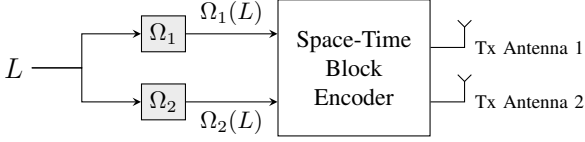


Fig. 1: Block Diagram of a USTLD Transmitter

To achieve labelling diversity, USTLD systems use constellations with two different binary mappings to encode the information to be transmitted. That is, an  $m$ -bit information codeword (or label)  $L$  is passed through binary mappers  $\Omega_1$  and  $\Omega_2$  to produce the respective symbols  $\Omega_1(L)$  and  $\Omega_2(L)$ . This process is illustrated in Fig. 1 for a single codeword. The USTLD STBC system model described by [1] considers a MIMO structure with two transmit antennas and  $N_R$  receive antennas. Two codewords,  $L^{(1)}$  and  $L^{(2)}$ , are transmitted over consecutive time slots. When encoding these codewords, binary mapper  $\Omega_t$  is used during the  $t$ -th time slot, where  $t \in [1 : 2]$ . Thus, the  $N_R \times 1$  received signal vector,  $\mathbf{y}$ , in time slot  $t$  is given by

$$\mathbf{y}_t = \sqrt{\frac{\rho}{2}} \left[ \mathbf{h}_{t,1} \Omega_t(L^{(1)}) + \mathbf{h}_{t,2} \Omega_t(L^{(2)}) \right] + \mathbf{n}_t \quad (1)$$

In (1),  $\rho = \frac{E_s}{E_\Omega E_n}$  is the total average SNR at the transmitter, wherein  $E_s$  is the transmit energy per symbol and  $E_\Omega$  is the average energy of the constellation (used to normalise the symbol power before transmission).  $E_n$  is the expected energy of additive white Gaussian noise at the receiver, which is represented by  $N_R \times 1$  vector  $\mathbf{n}$ . Each independent entry in  $\mathbf{n}$  follows a complex normal distribution with zero mean and variance  $\frac{E_n}{2}$  per dimension. The  $N_R \times 1$  vector  $\mathbf{h}_{t,u}$ ,  $t, u \in [1 : 2]$ , represents the multipath fading experienced by the symbol transmitted from antenna  $u$  during time slot  $t$ . The fading is assumed to be frequency flat and follow a Rayleigh amplitude distribution with zero mean and unit variance. Fading may be either fast or quasi-static over the duration of the two time slots. The phase distribution of both the noise and fading is assumed to be uniform.

At the receiver, maximum-likelihood detection is used to estimate the transmitted information codewords. Assuming that perfect channel state information is available at the receiver, detection may be described according to

$$\tilde{L}^{(1)}, \tilde{L}^{(2)} = \arg \min_{\tilde{L}^{(1)}, \tilde{L}^{(2)} \in [0:M-1]} \mathcal{D}_1 + \mathcal{D}_2, \quad (2)$$

where

$$\mathcal{D}_t = \left\| \mathbf{y}_t - \sqrt{\frac{\rho}{2}} \sum_{u=1}^2 \mathbf{h}_{t,u} \Omega_t(\tilde{L}^{(u)}) \right\|^2, \quad t \in [1 : 2] \quad (3)$$

In (2) and (3), the estimated codewords are denoted as  $\tilde{L}^{(1)}$  and  $\tilde{L}^{(2)}$ .  $\tilde{L}^{(1)}$  and  $\tilde{L}^{(2)}$  represent candidate labels to be tested during the detection.

## III. MAPPER DESIGN

Based on the model described in Section II, the analytical union bound on the average bit error probability (ABEP) of a USTLD system has been derived in [1]. The resulting expression is

$$P_b(\rho) \leq \frac{1}{mM} \sum_{L=0}^{M-1} \sum_{\substack{\tilde{L}=0 \\ \tilde{L} \neq L}}^{M-1} \delta(L, \tilde{L}) P(L \rightarrow \tilde{L}), \quad (4)$$

where  $M = 2^m$  is the number of points in the signal constellation and  $\delta(L, \tilde{L})$  is the number of bit errors between the transmitted label  $L$  and estimated label  $\tilde{L}$ .  $P(L \rightarrow \tilde{L})$  is the pairwise error probability (PEP) of  $L$  being detected erroneously as  $\tilde{L}$ . It is shown in [1] that the PEP is given by

$$P(L \rightarrow \tilde{L}) = \frac{1}{4r} \prod_{t=1}^2 \left( 1 + \frac{\rho d_t^2}{8} \right)^{-N_R} + \frac{1}{2r} \sum_{s=1}^{r-1} \prod_{t=1}^2 \left( 1 + \frac{\rho d_t^2}{8 \sin^2\left(\frac{s\pi}{2r}\right)} \right)^{-N_R}, \quad (5)$$

where  $r$  is an arbitrarily large integer  $r > 10$  and  $d_t = |\Omega_t(L) - \Omega_t(\tilde{L})|$ ,  $t \in [1 : 2]$ , is the Euclidean distance between the constellation points represented by  $L$  and  $\tilde{L}$  when mapped using  $\Omega_t$ . For details on the derivation of (4) and (5), the reader is referred to [1, Eq. (3)–(10)].

The authors of [1] show that at high SNRs,  $\frac{\rho d_t^2}{8} \gg 1$ ,  $t \in [1 : 2]$ . Under these conditions, the PEP in (5) may be approximated as

$$P(L \rightarrow \tilde{L}) \approx \frac{1}{4r} \left( \frac{\rho d_1^2}{8} \cdot \frac{\rho d_2^2}{8} \right)^{-N_R} + \frac{1}{2r} \sum_{s=1}^{r-1} \left( \frac{\rho d_1^2}{8 \sin^2\left(\frac{s\pi}{2r}\right)} \cdot \frac{\rho d_2^2}{8 \sin^2\left(\frac{s\pi}{2r}\right)} \right)^{-N_R} \quad (6)$$

The result in (6) indicates that the ABEP of USTLD systems at high SNRs is dominated by the product Euclidean distance,  $d_1 d_2$ . Hence, the minimum product Euclidean distance sets the error floor, providing a metric that may be used to evaluate the extent to which a pair of mappers  $\Omega_1$  and  $\Omega_2$  achieve LD. This metric is given by

$$\Psi(\Omega_1, \Omega_2) = \min_{\substack{L, \tilde{L} \in [0:M-1] \\ L \neq \tilde{L}}} \left[ \prod_{t=1}^2 |\Omega_t(L) - \Omega_t(\tilde{L})| \right] \quad (7)$$

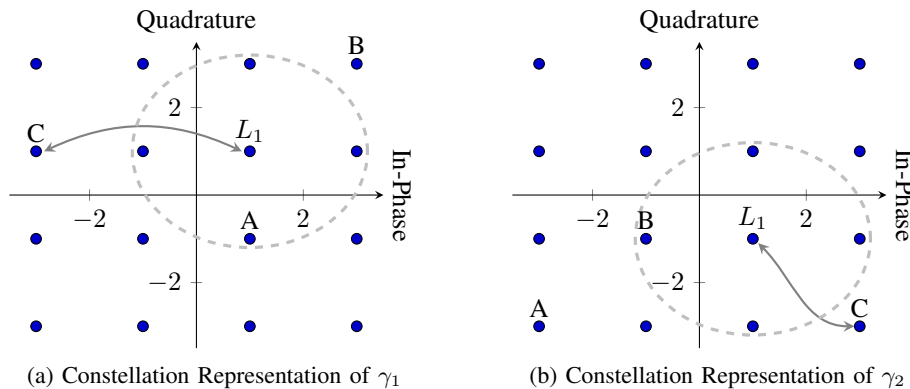


Fig. 2: Illustration of Hypersphere Swap Crossover

Higher values of  $\Psi(\Omega_1, \Omega_2)$  indicate that more LD is achieved. Thus, the objective of mapper design is to maximise  $\Psi(\Omega_1, \Omega_2)$ . In this paper, the proposed GA takes in a base mapper,  $\Omega_1$ , and produces an appropriate secondary mapper,  $\Omega_2$  that achieves LD. This process may be described as an instance of the QAP [1], [6].

#### A. The Quadratic Assignment Problem

The QAP is an optimisation problem that describes the challenge of assigning each of  $M$  variables to one of  $M$  locations, in order to optimise a given cost function [17]. In the context of mapper design for an  $M$ -ary constellation, the variables in question are each of the binary labels  $L \in [0 : M - 1]$  and the locations are the constellation points [6]. The cost function for this optimisation is given by (7). For this application, the QAP has  $M!$  complexity which exceeds  $10^{13}$  for  $M > 16$ . A genetic algorithm is applied to find a solution to such a computationally expensive problem, as described in the next subsection.

#### B. Proposed Genetic Algorithm

GAs mimic the process of evolution and natural selection to solve complex problems in an iterative manner. The GA designed for generating USTLD mappers is as follows:

1) *Genetic Coding*: The first step of the GA is to represent a candidate solution to the problem as a chromosome,  $\gamma$ . Information is encoded within the chromosome by individual values referred to as genes. For this application, each gene  $\ell_i, i \in [0 : M - 1]$ , represents a point on the constellation and the value contained within the gene is the label associated with that constellation point. Hence the chromosome is defined as

$$\gamma = [\ell_0 \ \ell_1 \ \dots \ \ell_{M-1}] \quad (8)$$

The set of  $p$  chromosomes representing the population of candidate mappers is denoted by  $\mathcal{P}$ . The initial population,  $\mathcal{P}^{(0)}$ , is constructed from using a random selection of  $p$  chromosomes. Additionally, for constellations where existing heuristic-based mappers are available, these mappers are encoded as chromosomes and added to the initial population. This ensures that the GA will always either match or improve

upon the heuristic-based design. Since each chromosome can be represented geometrically by a constellation with a given binary mapping, the terms ‘chromosome’ and ‘constellation’ will occasionally be used interchangeably in the following sections.

2) *Crossover and Mutation*: The most important step of the GA is the crossover [17]. During crossover, ‘parent’ chromosomes from the population are used to generate ‘offspring’ chromosomes that retain the most desirable properties from the parents. Various crossover techniques for optimising constellation assignments were investigated in [16], however these are not suitable for USTLD mapper design. In [16], the GA repositions constellation points (each with its associated label) in order to achieve optimisation. By contrast, when designing  $\Omega_2$  to achieve LD in a USTLD system, the positions of the constellation points are fixed by the constellation used by  $\Omega_1$ . This constraint requires that a new crossover operation be developed for the proposed GA.

The crossover operation designed for the proposed GA is called the hypersphere swap crossover (HSX), and is best illustrated by example. Consider two parent chromosomes,  $\gamma_1$  and  $\gamma_2$ , which produce two offspring chromosomes,  $\bar{\gamma}_1$  and  $\bar{\gamma}_2$ , using HSX. A label  $L_1$  is selected at random, and is located in gene  $\ell^{\gamma_1, L_1}$  in the first parent chromosome and gene  $\ell^{\gamma_2, L_1}$  in the second parent chromosome. A hypersphere of radius  $R$  is then constructed, and projected around the points corresponding to  $L_1$  on each of the constellations defined by the parent chromosomes. A second label  $L_2$  is then selected at random, such that the points corresponding to  $L_2$  fall outside the hypersphere. This ensures that the points corresponding to labels  $L_1$  and  $L_2$  are sufficiently far apart on both constellations. Offspring  $\bar{\gamma}_1$  is then generated by swapping the genes containing  $L_1$  and  $L_2$  in parent chromosome  $\gamma_1$ , i.e.  $\ell^{\bar{\gamma}_1, L_1} = \ell^{\gamma_1, L_2}$  and  $\ell^{\bar{\gamma}_1, L_2} = \ell^{\gamma_1, L_1}$ .  $\bar{\gamma}_2$  is similarly generated from  $\gamma_2$ .

For clarity, this process is illustrated in Fig. 2, using a 16QAM constellation example. Figs. 2a and 2b respectively represent the mappings represented by the parent chromosomes that will undergo crossover. Following the process described above, the first label  $L_1$  is selected at random. A

hypersphere of radius  $R$  centred around  $L_1$  is constructed, such that the nearest adjacent neighbours to  $L_1$  are contained within the hypersphere. The projection of this hypersphere on each constellation is indicated by the dashed circle. Points A, B and C are shown as candidates for  $L_2$ . Both A and B are inappropriate for swapping with  $L_1$ , as A falls within the region defined by the hypersphere in the constellation corresponding to  $\gamma_1$  (see Fig. 2a). Similarly, B falls within the hypersphere in the constellation corresponding to  $\gamma_2$  (see Fig. 2b). Thus, C is the only candidate that meets the criteria for swapping according to the HSX. When implementing HSX in the GA for USTLD mapper design, performing only one swap does not produce offspring that are sufficiently different to their parents. For this reason, a  $k$ -point HSX ( $k$ -HSX) is implemented (i.e.  $k$  swaps are done per crossover). The hypersphere radius  $R$  should be chosen such that it encompasses less than half of the points when projected onto each constellation.

Mutation in the context of GAs is a probabilistic event that an offspring undergoes a further change after crossover. In the context of this GA, mutation occurs by swapping any two genes in the offspring chromosome. The authors emphasise that, unlike HSX, the swapping is not dependent on the parent chromosomes. The probability of a mutation occurring is denoted  $P_m$ .

3) *Evaluation of Chromosomes:* After offspring are generated and added to  $\mathcal{P}$ , “natural selection” is imitated. All chromosomes of the population in the  $n$ -th iteration,  $\mathcal{P}^{(n)}$  are evaluated according to a fitness function, and the  $p$  best chromosomes are selected to form the next generation population  $\mathcal{P}^{(n+1)}$ . As stated previously, the fitness function is given by (7). The reader is reminded that  $\Omega_1$  is known, and that each chromosome in  $\mathcal{P}$  represents a candidate mapper for  $\Omega_2$ . Steps 2–3 of the proposed GA are summarised in Fig. 3.

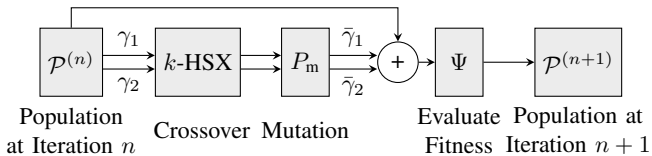


Fig. 3: Block Diagram of Proposed Genetic Algorithm

4) *Termination:* Termination of a GA occurs when the population  $\mathcal{P}$  is deemed to contain an optimal solution, or if the algorithm determines that no feasible solution can be found. As in [14]–[16], the proposed GA determines that an optimal solution has been found when all chromosomes in  $\mathcal{P}$  have converged to the same fitness value, i.e.  $\Psi(\Omega_1, \gamma_a) = \Psi(\Omega_1, \gamma_b), \forall \gamma_a, \gamma_b \in \mathcal{P}$ . In this case, all chromosomes in  $\mathcal{P}$  are regarded as optimal. The algorithm is constrained to only perform a maximum of  $n_{\max}$  iterations, after which it is assumed that the GA will not converge. In this case, the GA output is the chromosome in  $\mathcal{P}$  with the highest fitness, and is regarded as suboptimal. Setting  $n_{\max} \ll M^5$  ensures that the GA is less computationally expensive than the branch-and-bound QAP solvers discussed in [6].

## IV. RESULTS AND DISCUSSION

In this section, the output of the proposed GA for USTLD mapper design, denoted  $\Omega_2^{\text{GA}}$ , is evaluated. As in [1], the error performance benefits of  $2 \times N_R$  USTLD systems are demonstrated by comparing them to  $2 \times N_R$  Alamouti STBC systems [19]. This provides a fair comparison, as both systems have the same antenna array structure and spectral efficiency. It is also noted that, due to the similar structures of Alamouti STBC and USTLD systems, the union bound error performance of the Alamouti STBC system can be obtained from (4) by setting  $d_1 = d_2$ . All applications of the GA use parameters:  $p = 8$  and  $P_m = 10\%$ . When implementing the  $k$ -HSX,  $k = \frac{M-4}{2}$  is chosen and offspring are produced by all possible combinations of parent chromosomes within  $\mathcal{P}$ . For MPSK and APSK constellations, the hypersphere radius  $R = 1$  is selected. This is increased to  $R = 3$  for MQAM. The maximum number of iterations for the GA is set as  $n_{\max} = 10^4$  for 16-ary constellations and  $n_{\max} = 10^6$  for larger constellations. All binary mappings are represented by their decimal equivalent for brevity.

### A. Square Constellations: MQAM

First, the output of the GA is tested with 16QAM and 64QAM constellations. In the case of 16QAM, the algorithm output is benchmarked against the mappers found in [1], [5] and [6]. These are denoted  $\Omega_2^{[1]}$ ,  $\Omega_2^{[5]}$  and  $\Omega_2^{[6]}$  respectively. Evaluating the quality of these mappers according to (7),  $\Psi(\Omega_1, \Omega_2^{[1]}) = \Psi(\Omega_1, \Omega_2^{[5]}) = \Psi(\Omega_1, \Omega_2^{[6]}) = 8.0$ . The GA converges to chromosomes with fitness  $\Psi(\Omega_1, \Omega_2^{\text{GA}}) = 8.0$ . Thus, it does not improve upon existing 16QAM mappers. In the case of 64QAM, the benchmark mappers are found in [1] and [5] and have fitness  $\Psi(\Omega_1, \Omega_2^{[1]}) = 4.0$  and  $\Psi(\Omega_1, \Omega_2^{[5]}) = 8.0$ . The GA is found to converge to  $\Psi(\Omega_1, \Omega_2^{\text{GA}}) = 8.0$ , again matching – but not improving upon – the best available heuristic-based design.

### B. Circular Constellations: MPSK and APSK

Next, the output of the proposed GA for 32PSK is considered. As the algorithmic approach of [6] is computationally infeasible for  $M > 16$ , the benchmark mapper for comparison is the heuristic-based design found in [1]. This symmetry-based heuristic is to swap alternate pairs of diametrically opposite constellation points across the origin [1], and the mapper it produces is denoted  $\Omega_2^{[1]}$ .  $\Omega_1$  selected as a pseudo-gray mapper.  $\Omega_1$ ,  $\Omega_2^{[1]}$  and the output of the GA,  $\Omega_2^{\text{GA}}$ , are illustrated in Fig. 4. These mappers have fitness scores of  $\Psi(\Omega_1, \Omega_2^{[1]}) = 0.0384$  and  $\Psi(\Omega_1, \Omega_2^{\text{GA}}) = 0.2178$ . The curves shown in Fig. 5 show the theoretical performance of these systems in a fast fading channel. These results are verified by Monte Carlo simulations using the system model described in Section II. These results indicate that the proposed mapper achieves significantly more LD than the heuristic mapper, as indicated by the  $\approx 8$ dB diversity gain at a BER of  $10^{-6}$ . This is expected, since  $\Psi(\Omega_1, \Omega_2^{\text{GA}})$  is an order of magnitude greater than  $\Psi(\Omega_1, \Omega_2^{[1]})$ .

TABLE I: 16APSK Constellation Points and Label Assignments

(a) 11+5 APSK [18]				(b) Asymmetric 16APSK [15]				(c) Single Symmetry 16APSK [15]			
Radius	Phase	$\Omega_1$	$\Omega_2^{GA}$	Radius	Phase	$\Omega_1$	$\Omega_2^{GA}$	Radius	Phase	$\Omega_1$	$\Omega_2^{GA}$
0.5501	0.0000	10	7	0.9593	4.7453	1	10	0.9627	2.3592	1	4
	1.2566	13	4		3.1109	5	5		1.2107	5	6
	2.5133	15	11		1.5490	9	14		-2.3592	9	2
	3.7699	6	0		0.4687	13	3		-1.2107	13	15
	5.0265	8	1								
1.1476	0.0000	7	13	1.000	5.0872	0	4	1.0000	2.5650	0	11
	0.5712	3	12		4.3400	2	13		2.0128	2	14
	1.1424	5	8		3.7447	3	1		1.7317	3	1
	1.7136	4	2		3.4121	4	11		1.4188	4	9
	2.2848	11	9		2.7071	6	8		0.8849	6	12
	2.8560	0	14		2.2326	7	6		0.5372	7	3
	3.4272	9	3		1.8925	8	2		-2.5650	8	13
	3.9984	14	6		1.2567	10	0		-2.0128	10	8
	4.5696	1	10		1.0438	11	7		-1.7317	11	7
	5.1408	12	5		0.7340	12	9		-1.4188	12	0
5.7120	2	15	0.2205	14	15	-0.8849	14	5			
				0.0699	15	12	-0.5372	15	10		
$\Psi(\Omega_1, \Omega_2^{GA}) = 0.6766$				$\Psi(\Omega_1, \Omega_2^{GA}) = 0.0981$				$\Psi(\Omega_1, \Omega_2^{GA}) = 0.4020$			

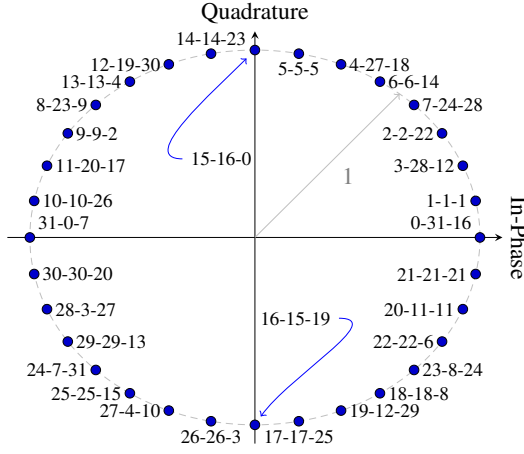
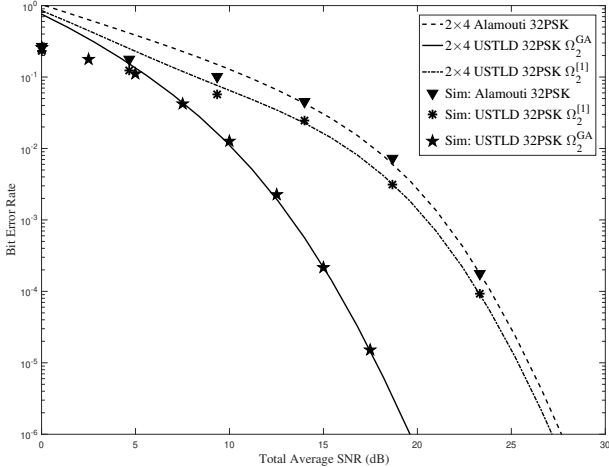

 Fig. 4: 32PSK Constellation. Key:  $\Omega_1 - \Omega_2^{[1]} - \Omega_2^{GA}$ 


Fig. 5: Bit Error Performance of 32PSK Alamouti and USTLD Systems

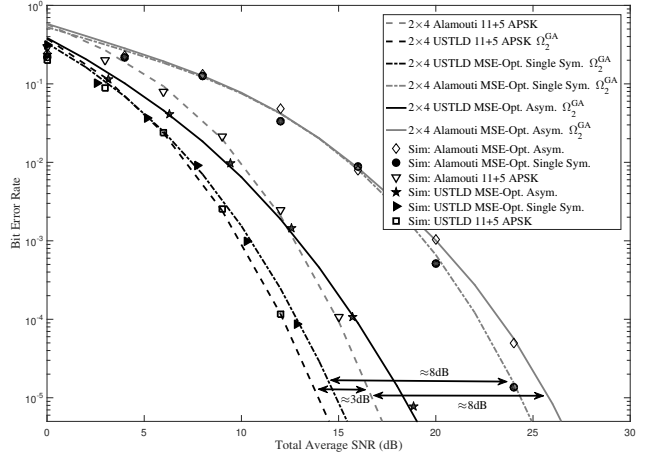


Fig. 6: Bit Error Performance of 16APSK Alamouti and USTLD Systems

Finally, the proposed algorithm is applied to three 16APSK constellations that do not exhibit diagonal symmetry. No existing USTLD mapper design heuristics are directly applicable to these constellations. Additionally, as they are not diagonally symmetrical, the heuristic-based MPSK mapper design technique proposed by [1] cannot be modified and applied to these constellations. The 16APSK constellations considered are:

- 1) The optimised 11+5 APSK constellation proposed by [18], which has 11 points in its outer ring and 5 points in its inner ring.
- 2) The asymmetric mean-square error (MSE) optimised 16APSK constellation proposed by [15].
- 3) The MSE-optimised 16APSK constellation with a single degree of symmetry across the horizontal axis, which was also proposed by [15]. The work in [15] shows that

this single symmetry constellation is more optimal than the asymmetric case.

For each of these constellations, a pseudo-gray binary mapping is selected for  $\Omega_1$  and the proposed GA is used to generate a secondary mapper to achieve LD,  $\Omega_2$ . Table I summarises the constellation points (represented in polar coordinates), mappings and fitness score for each of these constellations, calculated using (7). The quality of these mappers are again evaluated by comparing to the Alamouti STBC system, and the results are presented in Fig. 6. These results show that the GA-designed mappers are able to improve the error performance of the asymmetric and single symmetry constellations proposed by [15] by approximately 8dB at a BER of  $10^{-5}$ . In addition, the performance of the 11+5 APSK constellation proposed by [18] is improved by approximately 3dB in the same region.

## V. CONCLUSION

Existing design techniques for USTLD mappers are limited to approaches that either rely on symmetry-based heuristics, or algorithms that are too computationally expensive to be applied to constellations where  $M > 16$ . This paper proposes a new mapper design technique based on GAs, which can be applied to constellations of any shape and size. The algorithm was tested on 16QAM, 64QAM, 32PSK and non-diagonally-symmetric 16APSK constellations. Results presented indicate that the proposed mappers match the best existing mappers for 16QAM and 64QAM; and out-perform the best existing 32PSK mapper by a diversity gain of 8dB. When applied to a USTLD system, the proposed 11+5 APSK mapper is shown to achieve a diversity gain of 3dB when compared to an Alamouti STBC system. In addition, under the same conditions, the asymmetric and single symmetric 16APSK constellation LD mappers both produced a diversity gain of 8dB.

Future works in this area may consider even larger constellations, look at developing improved metrics for determining the fitness of mappers, as well as investigating other crossover operators, mutation operators and termination conditions for the proposed GA.

## REFERENCES

- [1] H. Xu, K. Govindasamy, and N. Pillay, "Uncoded Space-Time Labelling Diversity," *IEEE Commun. Lett.*, vol. 20, no. 8, pp. 1511–1514, Aug. 2016.
- [2] Y. Huang and J. A. Ritcey, "Optimal constellation labeling for iteratively decoded bit-interleaved space-time coded modulation," *IEEE Trans. Inf. Theory*, vol. 51, no. 5, pp. 1865–1871, May 2005.
- [3] —, "Improved 16-QAM constellation labeling for BI-STCM-ID with the Alamouti scheme," *IEEE Commun. Lett.*, vol. 9, no. 2, pp. 157–159, Feb. 2005.
- [4] M. Krasicki, "Essence of 16-QAM labelling diversity," *IET Electronics Lett.*, vol. 49, no. 8, pp. 567–569, Apr. 2013.
- [5] K. G. Seddik, A. S. Ibrahim, and K. J. R. Liu, "Trans-Modulation in Wireless Relay Networks," *IEEE Commun. Lett.*, vol. 12, no. 3, pp. 170–172, Mar. 2008.
- [6] H. Samra, Z. Ding, and P. Hahn, "Symbol Mapping Diversity Design for Multiple Packet Transmissions," *IEEE Trans. Commun.*, vol. 53, no. 5, pp. 810–817, May 2005.
- [7] K. Govindasamy, H. Xu, and N. Pillay, "Space-time block coded spatial modulation with labeling diversity," *Int. J. Commun. Syst.*, vol. 31, no. 1, e3395, Sep. 2017. DOI: 10.1002/dac.3395.
- [8] N. Pillay and H. Xu, "Uncoded Space-Time Labeling Diversity— Application of Media-based Modulation with RF Mirrors," *IEEE Commun. Lett.*, vol. 22, no. 2, pp. 272–275, 2018.
- [9] S. S. Patel, T. Quazi, and H. Xu, "Error performance of Uncoded Space Time Labelling Diversity in spatially correlated Nakagami-q channels," *Int. J. Commun. Syst.*, vol. 31, no. 12, e3720, Aug. 2018. DOI: 10.1002/dac.3720.
- [10] —, "Full MIMO Uncoded Space Time Labelling Diversity with Low-Complexity Detection," under review, *IET Commun.*, 2017.
- [11] T. Quazi and H. Xu, "SSD-enhanced uncoded space-time labeling diversity," *Int. J. Commun. Syst.*, vol. 31, no. 11, e3592, Jul. 2018. DOI: 10.1002/dac.3592.
- [12] D. E. Goldberg, *Genetic Algorithms in Search, Optimization and Machine Learning*. Addison-Wesley, 1989.
- [13] Z. H. Ahmed, "An Improved Genetic Algorithm using Adaptive Mutation Operator for the Quadratic Assignment Problem," in *Proc. 38th Int. Conf. Telecomm. Signal Process. (TSP)*, Prague, Czech Republic, 2015. DOI: 10.1109/TSP.2015.7296481.
- [14] M. Anedda, A. Meloni, and M. Murrioni, "64-APSK Constellation and Mapping Optimization for Satellite Broadcasting Using Genetic Algorithms," *IEEE Trans. Broadcast.*, vol. 62, no. 1, pp. 1–9, 2016.
- [15] A. Meloni and M. Murrioni, "On the genetic optimization of APSK constellations for satellite broadcasting," in *Proc. IEEE Int. Symp. Broadband Multimedia Syst. Broadcast. (BMSB)*, Beijing, China, 2014, pp. 1–6.
- [16] A. Angioi, M. Lixia, and M. Murrioni, "Optimized APSK bit allocation for Satellite Communication," in *Proc. 5th ASMS 11th SPSC Workshop*, Cagliari, Italy, 2010, pp. 407–412.
- [17] A. Misevicius and E. Guogis, "Computational Study of Four Genetic Algorithm Variants for Solving the Quadratic Assignment Problem," in *Information and Software Technologies*, T. Skersys, R. Butleris, and R. Butkiene, Eds., Berlin, Heidelberg: Springer Berlin Heidelberg, 2012, pp. 24–37, ISBN: 978-3-642-33308-8.
- [18] X. Chen and H. Yang, "Optimization of MAPSK," in *11th Int. Conf. Advanced Commun. Tech. (ICACT)*, Phoenix Park, South Korea, 2009, pp. 1071–1072.
- [19] S. Alamouti, "A Simple Transmit Diversity Technique for Wireless Communications," *IEEE J. Sel. Areas Commun.*, vol. 16, no. 8, pp. 1451–1458, Oct. 1998.